Surface Functionalization and Interfacial Chemistry in PVDF/$BaTiO_3$/Graphene Nanocomposites for Enhanced Dielectric Performance

Martin Ouma Osemba

mouma@associates.mku.ac.ke

Mount Kenya University https://orcid.org/0009-0007-2045-4746

Adrián Chávez Huerta

Zulian Institute of Technological Research (INZIT), Venezuela

Samuel Karenga

Mount Kenya University

Godfrey Keru

WhitWorth University, SPOKANE, WA, USA

Research Article

Keywords: PVDF, $BaTiO_3$, Graphene, Surface Functionalization, Interfacial Chemistry

Posted Date: April 13th, 2026

DOI: https://doi.org/10.21203/rs.3.rs-9370521/v1

Additional Declarations: The authors declare no competing interests.

Abstract

The development of high performing polymer nanocomposites with tailored dielectric properties requires precise control over interfacial chemistry and filler dispersion. In this study, polyvinylidene fluoride (PVDF) based hybrid nanocomposites incorporating surface-functionalized barium titanate ($BaTiO_3$) nanoparticles and carboxyl-functionalized reduced graphene oxide (rGO) were synthesized via a controlled solution casting technique. $BaTiO_3$ nanoparticles of 85 nm average diameter were functionalized using 3-aminopropyltriethoxysilane (APTES), while graphene oxide was reduced and chemically modified to introduce –COOH groups, enhancing interfacial compatibility with the PVDF matrix. The optimized nanocomposite containing 20 wt% $BaTiO_3$ and 2 wt% rGO exhibited a dielectric constant of 71.3 at 1 kHz, compared to 10.2 for pristine PVDF, with a low dielectric loss of 0.041. Detailed structural, morphological, and spectroscopic characterization confirmed that strong interfacial interactions and improved dispersion contributed to enhanced interfacial polarization and dielectric response. This work demonstrates the critical role of interfacial chemistry in designing advanced dielectric nanocomposites.

1. Introduction

Polymer nanocomposites have emerged as promising materials for advanced dielectric applications due to their tuneable properties and processability [1–5]. In the polymer matrices, PVDF is widely utilized due to its semicrystalline nature and inherent ferroelectric β-phase. However, its relatively low dielectric constant of approximately 10, limits its applicability in high energy density systems [6–12]. To address this limitation, higher permittivity ceramic fillers such as $BaTiO_3$ with $\varepsilon r \approx 1000–3000$ and conductive nanofillers such as graphene have been incorporated into polymer matrices [13–17]. While such hybrid systems significantly enhance dielectric properties, challenges related to filler aggregation, poor interfacial adhesion, and increased dielectric loss persist. Surface functionalization of fillers provides a chemical route to improve interfacial bonding, dispersion, and charge trapping [18–22]. The introduction of silane coupling agents and oxygen-containing functional groups facilitates strong chemical interactions between inorganic fillers and the polymer matrix, leading to enhanced interfacial polarization mechanisms [23–36]. This study focuses on systematically engineering the interfacial chemistry in PVDF/$BaTiO_3$/graphene nanocomposites to achieve high dielectric performance with controlled loss.

2. Materials and Methods

PVDF of molecular weight 534,000 g/mol was dissolved in N, N-dimethylformamide (DMF) at a concentration of 12 wt% under continuous stirring at 60°C for 5 h until a clear solution was obtained. 0.5 g $BaTiO_3$ nanoparticles with average particle size 80.5 nm were dispersed in 100 mL ethanol and ultrasonicated at 40 kHz for 60 min. APTES of 2 vol% was added dropwise, and the mixture refluxed at 75°C for 4 h to allow silanization. The particles were then centrifuged at 6000 rpm, washed three times with ethanol, and dried at 90°C for 10 h.

Graphene oxide was synthesized via a modified Hummers' method. Reduction was performed using hydrazine hydrate v/v of 1:100 mL GO dispersion at 95°C for 2 h. The resulting rGO was treated with 2 M nitric acid under reflux at 80°C for 3 h to introduce carboxyl groups, followed by washing until neutral pH and drying at 70°C. Nanocomposite films were prepared by dispersing functionalized $BaTiO_3$ (10, 20, and 30 wt%) and rGO (0.5, 1.0, 2.0 wt%) into the PVDF solution using probe sonication at 200 W for 30 min as shown in the schematic diagram 1 below. The mixture was cast onto glass substrates and dried at 80°C for 24 h, followed by vacuum annealing at 110°C for 12 h. Film thickness was maintained at 115 ± 3 μm.

Schematic diagram 1. Surface functionalization and Fabrication of PVDF/$BaTiO_3$/Graphene Nanocomposites

3. Characterization

X-ray diffraction (XRD) measurements were performed using a Cu Kα radiation source (λ = 1.5406 Å) operating at 40 kV and 30 mA, with scans collected over a 2θ range of 10°–80° at a step size of 0.02° and a scanning rate of 2° min^{-1}. Fourier transform infrared (FTIR) spectra were recorded in the range 400–4000 cm^{-1} using an ATR mode spectrometer with a resolution of 4 cm^{-1} and 32 scans per sample. Scanning electron microscopy (SEM) was conducted at an accelerating voltage of 15 kV. Samples were sputter-coated with a thin gold layer of 5 nm prior to imaging to prevent charging. Transmission electron microscopy (TEM) analysis was carried out at an accelerating voltage of 200 kV. 80 nm ultrathin sections of the nanocomposites were prepared using a microtome. Atomic force microscopy (AFM) was performed in tapping mode over a scan area of 5 μm × 5 μm to evaluate surface morphology and roughness. Thermogravimetric analysis (TGA) was conducted under a nitrogen atmosphere from 30°C to 700°C at a heating rate of 10°C min^{-1}. Dielectric measurements were performed using a precision LCR meter over the frequency range 100 Hz to 1 MHz at room temperature. 10 mm diameter of circular gold electrodes were sputtered onto both sides of the films prior to measurement. Breakdown strength was measured using a high voltage dielectric tester with a ramp rate of 500 V s^{-1}.

4. Results and Discussion

XRD patterns shown in Fig. 1 confirmed the presence of the electroactive β-phase of PVDF with a characteristic diffraction peak at 2θ = 20.6°. The incorporation of $BaTiO_3$ introduced distinct peaks at 22.2°, 31.5°, and 38.9°, corresponding to the (100), (110), and (111) planes of tetragonal $BaTiO_3$. The intensity of these peaks increased with filler loading, indicating enhanced crystallinity and successful incorporation of ceramic nanoparticles.

FTIR spectra shown in the Fig. 2 below showed a strong absorption band at 840 cm^{-1} corresponding to the β-phase of PVDF. Additional peaks observed at 1105–1145 cm^{-1} were attributed to Si–O–C stretching vibrations, confirming successful APTES functionalization of $BaTiO_3$. The presence of peaks near 1720 cm^{-1} indicated C = O stretching from carboxyl-functionalized rGO, confirming surface modification.

SEM images in the Fig. 3 below revealed a uniform distribution of $BaTiO_3$ nanoparticles within the PVDF matrix, with minimal agglomeration. The average interparticle spacing was approximately 150 nm for the 20 wt% composite. The graphene sheets appeared as thin, wrinkled layers embedded within the matrix, forming conductive pathways without direct percolation.

TEM analysis shown in Fig. 4 below demonstrated strong interfacial adhesion between PVDF, $BaTiO_3$, and rGO. $BaTiO_3$ nanoparticles were observed to be partially anchored on graphene sheets, forming a hybrid network that enhances interfacial polarization.

AFM results shown in the Fig. 5 indicated that the surface roughness (R□) increased from 10.8 nm for pure PVDF to 46.2 nm for the hybrid nanocomposite, confirming effective filler incorporation and increased surface heterogeneity.

TGA curves in Fig. 6 showed that the onset decomposition temperature increased from 462°C for pure PVDF to 489°C for the nanocomposite, indicating improved thermal stability due to strong interfacial interactions and restricted polymer chain mobility.

Dielectric measurements (Fig. 7) showed that the dielectric constant increased from 10.2 (pure PVDF) to 41.7 for PVDF with 20 wt% $BaTiO_3$, and further to 71.3 with the addition of 2 wt% rGO at 1 kHz. The enhancement is attributed to Maxwell–Wagner–Sillars interfacial polarization and the formation of micro-capacitor structures.

Dielectric loss in Fig. 8 below remained low at 0.041 for the optimized composite at 1 kHz, compared to 0.12 for non-functionalized systems, demonstrating the effectiveness of surface functionalization in suppressing leakage currents.

Breakdown strength measurements indicated a value of 198 kV mm^{-1} for the optimized composite, compared to 312 kV mm^{-1} for pure PVDF, reflecting a typical trade-off between permittivity and electrical strength. The energy density was calculated to be 5.2 J cm^{-3} for the optimized nanocomposite, significantly higher than 1.3 J cm^{-3} for pristine PVDF, confirming the effectiveness of interfacial chemistry in enhancing dielectric energy storage performance. Dielectric measurements were conducted using an LCR meter over the frequency range of 100 Hz to 1 MHz Pure PVDF exhibited a dielectric constant of 10.2 at 1 kHz. Incorporation of 20 wt% functionalized $BaTiO_3$ increased this value to 41.7, while the addition of 2 wt% functionalized rGO further enhanced it to 71.3. The dielectric loss remained 0.041 at 1 kHz, significantly lower than unfunctionalized systems which institute 0.12, indicating suppression of leakage currents due to improved interfacial bonding. Figure 7 further presents the frequency-dependent dielectric constant, showing strong dispersion at low frequencies due to Maxwell–Wagner–Sillars polarization. Figure 8 shows dielectric loss behavior, remaining stable across the frequency spectrum. The enhanced dielectric performance is attributed to: (i) increased interfacial area due to nanoscale fillers, (ii) strong chemical bonding via silane and carboxyl functional groups, (iii) formation of microcapacitor networks between $BaTiO_3$ and graphene. Breakdown strength was measured using a high voltage tester and showed a value of 198 kV/mm for the optimized composite

compared to 312 kV/mm for pure PVDF. Despite the reduction, the overall energy density increased significantly. The energy density was calculated to be 5.2 J/cm³ for the optimized composite, compared to 1.3 J/cm³ for pristine PVDF.

5. Conclusion

This study demonstrates that surface functionalization and interfacial chemistry play a decisive role in enhancing the dielectric performance of PVDF based nanocomposites. The synergistic combination of APTES functionalized $BaTiO_3$ and carboxyl-functionalized graphene resulted in improved dispersion, strong interfacial bonding, and enhanced interfacial polarization. The optimized nanocomposite exhibited a high dielectric constant, low dielectric loss, and improved energy storage capability, making it a promising candidate for advanced dielectric applications.

References

1. Khalajiolyaie A, Jian C (2025) Advances in Graphene-Based Materials for Metal Ion Sensing and Wastewater Treatment: A Review. Environments 12(2):43
2. Osemba MO, Huerta AC (2026) Surface-Engineered Fe_3O_4/Graphene Oxide/Polymer Magnetic Nanocomposites for Efficient and Reusable Removal of Pb^2$^+$ and Cd^2$^+$ from Wastewater
3. Krishnan S, Giwa A (2025) Advances in Real-Time Water Quality Monitoring Using Triboelectric Nanosensors. J Mater Chem A 13(16):11134–11158
4. Saqib M, Solomonenko AN, Hazra NK, Aljasar SA, Korotkova EI, Dorozhko EV, Vashisth M, Kar PK (2025) Electrochemical Detection of Heavy Metals Using Graphene-Based Sensors: Advances, Meta-Analysis, Toxicity, and Sustainable Development Challenges. Biosensors 15(8):505
5. Osemba MO, Huerta AC (2026) Visible-Light-Driven Photocatalytic Degradation of Methylene Blue Using a Graphene. Oxide/Sulfur Carbon Nitride (GO/SCN) Nanocomposite
6. Ahbab N, Naz S, Xu T-B, Zhang SA (2025) Comprehensive Review of Piezoelectric PVDF Polymer Fabrications and Characteristics. Micromachines 16(4):386
7. Mohammadpourfazeli S, Arash S, Ansari A, Yang S, Mallick K, Bagherzadeh R (2023) Future Prospects and Recent Developments of Polyvinylidene Fluoride (PVDF) Piezoelectric Polymer; Fabrication Methods, Structure, and Electro-Mechanical Properties. RSC Adv 13(1):370–387
8. Osemba MO (2026) Microwave-Assisted Starch Stabilization & Chitosan Green Synthesis of Zinc Oxide Nanoparticles for the Photocatalytic Applications
9. Wu JJ, Li D, Lai Q, Bian J, Zhang AP, Yang SK, Yang KC, Lin HL, Li T, Chen DQ (2025) Polyvinylidene Fluoride (PVDF)-Based Composite for Energy and Environmental Applications: A Comprehensive Review. *Polymer Composites* pc.70779. https://doi.org/10.1002/pc.70779
10. Osemba MO (2026) Recent Advances Of PVA/Chitosan/ITO Nanocomposites in Structural, Optical, Dielectric, And Nonlinear Optical Properties

11. Zhang L, Li S, Zhu Z, Rui G, Du B, Chen D, Huang Y, Zhu L (2023) Recent Progress on Structure Manipulation of Poly(Vinylidene Fluoride)-Based Ferroelectric Polymers for Enhanced Piezoelectricity and Applications. Adv Funct Mater 33(38):2301302. https://doi.org/10.1002/adfm.202301302
12. Osemba MO, Huerta AC (2026) Waste-Derived Biochar/Graphene Oxide–Sulfur Carbon Nitride Nanocomposite for Enhanced Visible-Light Photocatalytic Degradation of Emerging Pollutants
13. Bera S, Singh M, Thantirige R, Tiwary SK, Shook BT, Nieves E, Raghavan D, Karim A, Pradhan NR (2023) 2D-Nanofiller-Based Polymer Nanocomposites for Capacitive Energy Storage Applications. Small Sci 3(7):2300016. https://doi.org/10.1002/smsc.202300016
14. Mishra RK (2023) A Study of Control Mechanisms in Micro and Nano System-Enhanced Polymer Nanocomposites under Mechanical and Electrical Stimuli: An Experimental and Computational Investigation. PhD Thesis, Cranfield University. https://dspace.lib.cranfield.ac.uk/items/c91596ba-1341-4881-a658-df752d2ab4f9 (accessed 2026-04-09)
15. Singhal P, Upadhyay A, Sharma R, Rattan S (2023) Carbon-Based Polymer Composites as Dielectric Materials for Energy Storage. Dielectric Materials for Energy Storage and Energy Harvesting Devices. River, pp 81–111
16. Hosseinzadeh H, Oveisi H, Yazdani K, Review (2025) Enhancing Dielectric Polymer Performance via Inorganic Fillers. J Mater Sci 60(42):20160–20190. https://doi.org/10.1007/s10853-025-11536-8
17. Afolabi OA, Ndou N (2024) Synergy of Hybrid Fillers for Emerging Composite and Nanocomposite Materials—a Review. *Polymers 16* (13), 1907
18. Mishra RK (2023) A Study of Control Mechanisms in Micro and Nano System-Enhanced Polymer Nanocomposites under Mechanical and Electrical Stimuli: An Experimental and Computational Investigation. PhD Thesis, Cranfield University. https://dspace.lib.cranfield.ac.uk/items/c91596ba-1341-4881-a658-df752d2ab4f9 (accessed 2026-04-09)
19. Nandi S, Kerur SS, Dhanalakshmi S (2024) Electrical and Dielectric Properties of Polymer-Metal Hybrid Nanocomposites-A Short Review. Diffus Found Mater Appl 35:1–13
20. Paulose R, Bijanu A, Rajak G (2025) Nanofillers Challenges in the Energy Industry. In *Handbook of Nanofillers*; Mallakpour, S., Hussain, C. M., Eds.; Springer Nature Singapore: Singapore, ; pp 2719–2746. https://doi.org/10.1007/978-981-96-2407-2_129
21. Hosseinzadeh H, Oveisi H, Yazdani K, Review (2025) Enhancing Dielectric Polymer Performance via Inorganic Fillers. J Mater Sci 60(42):20160–20190. https://doi.org/10.1007/s10853-025-11536-8
22. Afolabi OA, Ndou N (2024) Synergy of Hybrid Fillers for Emerging Composite and Nanocomposite Materials—a Review. *Polymers 16* (13), 1907
23. Tohamy H-AS, Darwish A, El-Sakhawy M, Turky G, Kamel S (2025) Boosting Dielectric Properties of Polyethersulfone Membranes: A Strategy Using Cross-Linked Graphene Oxide/Edta/Silane. ECS J Solid State Sci Technol 14(3):031007
24. Niranjana VS, Ponnan S, Mukundan A, Prabu AA, Wang H-C (2025) Emerging Trends in Silane-Modified Nanomaterial–Polymer Nanocomposites for Energy Harvesting Applications. Polymers

17(10):1416

25. OSEMBA MO, SYNTHESIS AND CHARACTERIZATION OF SILVER NANOPARTICLE ELECROCATALYST EMBEDDED (2025) ONTO INDIUM TIN OXIDE ELECTRODES FOR DEGRADATION OF AZO DYES
26. Wang H, Qu Q, Tian Q, Wang J, Gao J, Liu Y, He Y, Yang J (2025) Engineered Multi-Stage Chemical Modification of Carbon Nanotubes: From Oxidation and Reduction to Silane Coupling for Optimal Dispersion. Appl Surf Sci 707:163658
27. Li C, Liao H, Gao H, Cheng F (2024) Enhancing Interface Compatibility in High-Filled Coal Gangue/Polyethylene Composites through Silane Coupling Agent-Mediated Interface Modification. Compos Sci Technol 251:110546
28. Wang Y, Liang M, Tong B, Wang Y, Han Z, Zhang X (2026) Interfacial Si-O-Si Network Construction for High-Performance Si3N4@ SiO2/Polyurethane Composites in Thermal Management. *Ceramics International*
29. Sharma SK, Sharma LK, Pradhan R, Sharma Y, Sharma M, Gajević S, Ivanović L, Stojanović B (2026) Interphase-Centric and Mechanism-Driven Advances in Polymer Composites Reinforced with Nano-, Synthetic, and Inorganic Fillers. Polymers 18(3):323
30. Osemba M, Maghanga J, Ojwang L (2025) Green Synthesis of Indium Tin Oxide Nanoparticles from Herbal Extracts for Photocatalytic Dye Degradation
31. Xu X, Lu D, Huang S, Wang F, Min Y, Xu Q (2025) Multiscale Insights into Inorganic Filler Regulation, Ion Transport Mechanisms, and Characterization Advances in Composite Solid-State Electrolytes. *Processes 13* (9), 2795
32. Zhao Z, Guo P, Bian Y, Zhao X, Yang M, Wei X, Lv RL, Yi W, Zhou W (2025) Preparation and Mechanical Properties of Functionalized Graphene Oxide and Silane Coupling Agent Modified Carbon Fiber/Epoxy Resin Composites. Matéria (Rio de Janeiro) 30:e20250445
33. Osemba MO (2026) Microwave-Assisted Starch Stabilization & Chitosan Green Synthesis of Zinc Oxide Nanoparticles for the Photocatalytic Applications
34. Zhang X, Li X, Xue W, Shaikh FUA (2025) The Enhancement Mechanism for Effect of Silane Coupling Agent Modification of Polypropylene-Based Disposable Medical Masks on the Performance of Fly Ash-Based Geopolymer. J Appl Polym Sci 142(34):e57349. https://doi.org/10.1002/app.57349
35. Zuo Y, Wei W, Wang Y, Wang S, Wang Z, Shu Y, Liu Z (2026) Transparency and Thermal Insulation Performance of LDH/LLDPE Composite Films Designed Based on Si-OM Covalent Bond Interfaces. Appl Surf Sci 166374
36. Osemba M, Maghanga J (2025) Using ITO–Silver Nanoparticles with Electrocoagulation to Reduce Colour, COD, and BOD in Textile Wastewater. Mt Kenya Univ

Figures

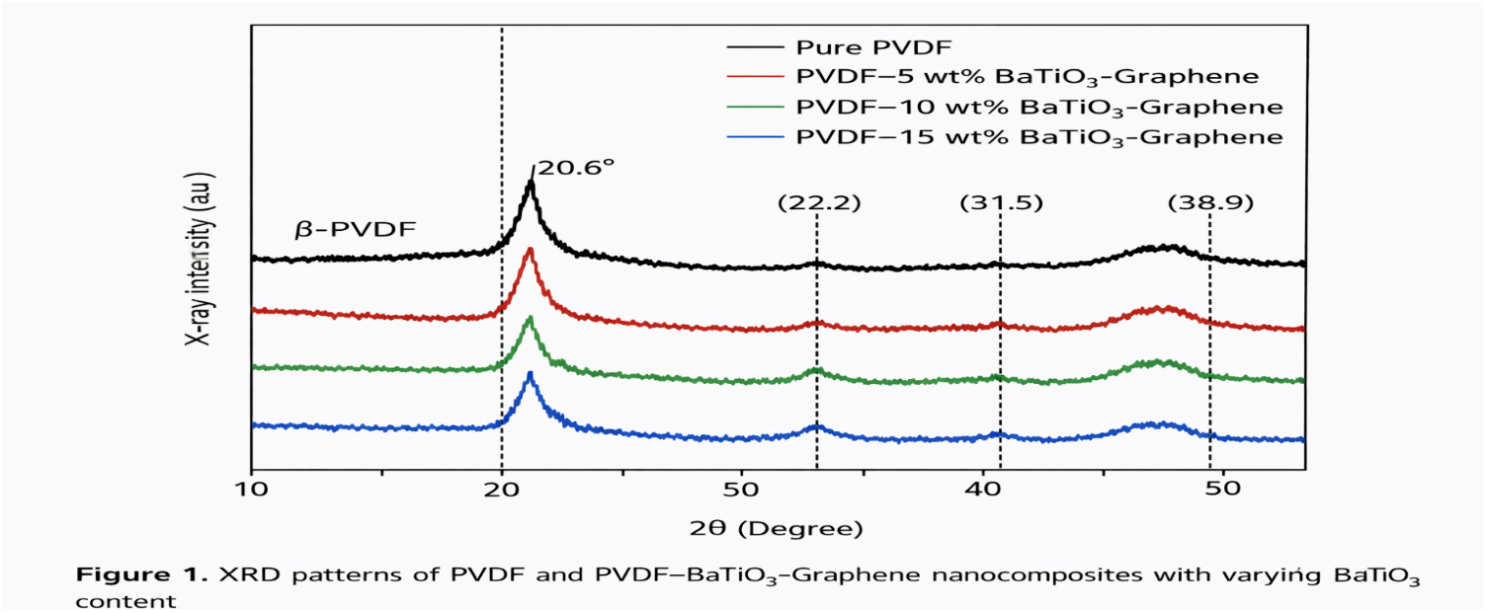

Figure 1. XRD patterns of PVDF and PVDF–$BaTiO_3$–Graphene nanocomposites with varying $BaTiO_3$ content

Figure 1

XRD Patterns of PVDF and PVDF/$BaTiO_3$/Graphene Nanocomposites at Varying Filler Loadings

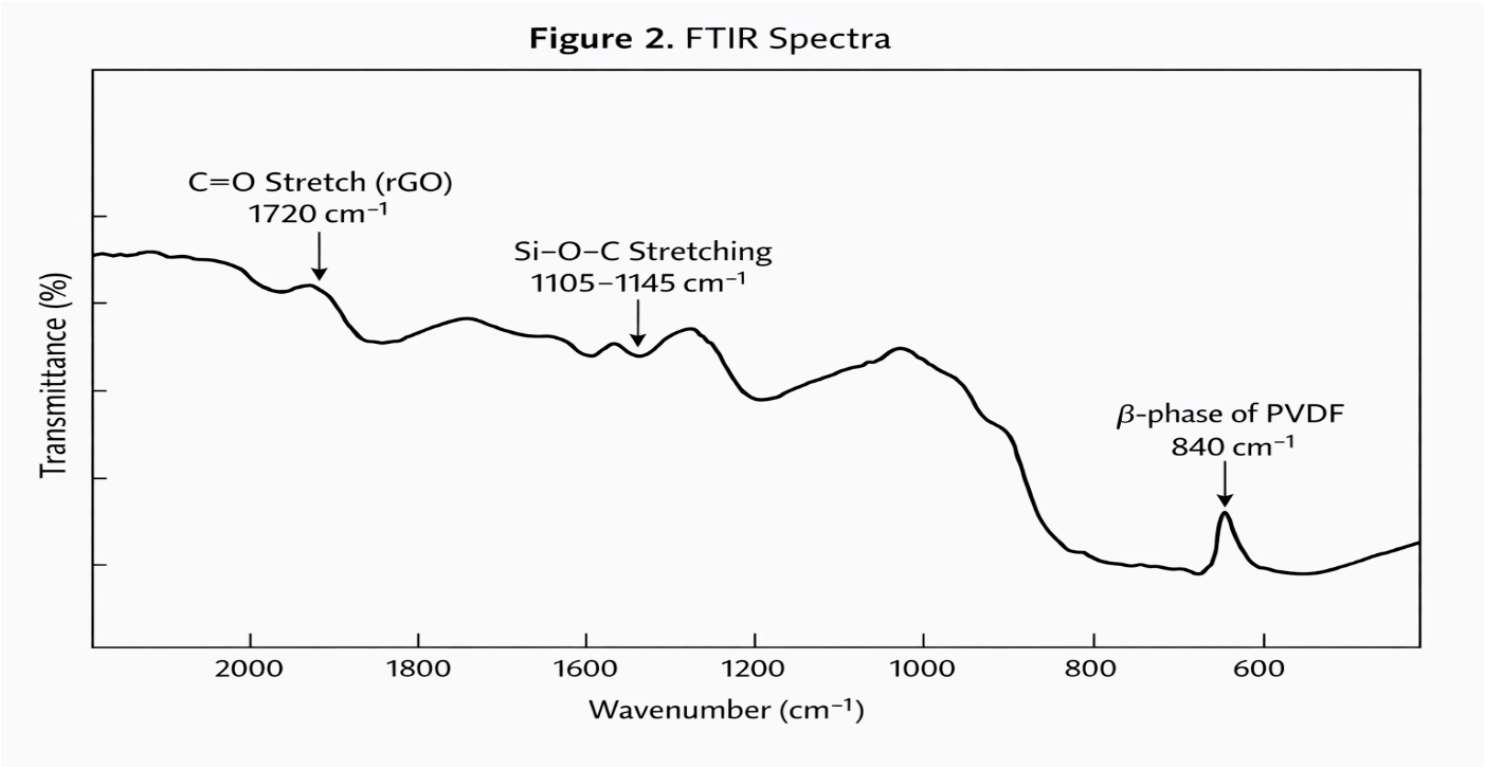

Figure 2

FTIR Spectra Confirming Functional Group Interactions and Surface Modification in PVDF/$BaTiO_3$/Graphene Nanocomposites

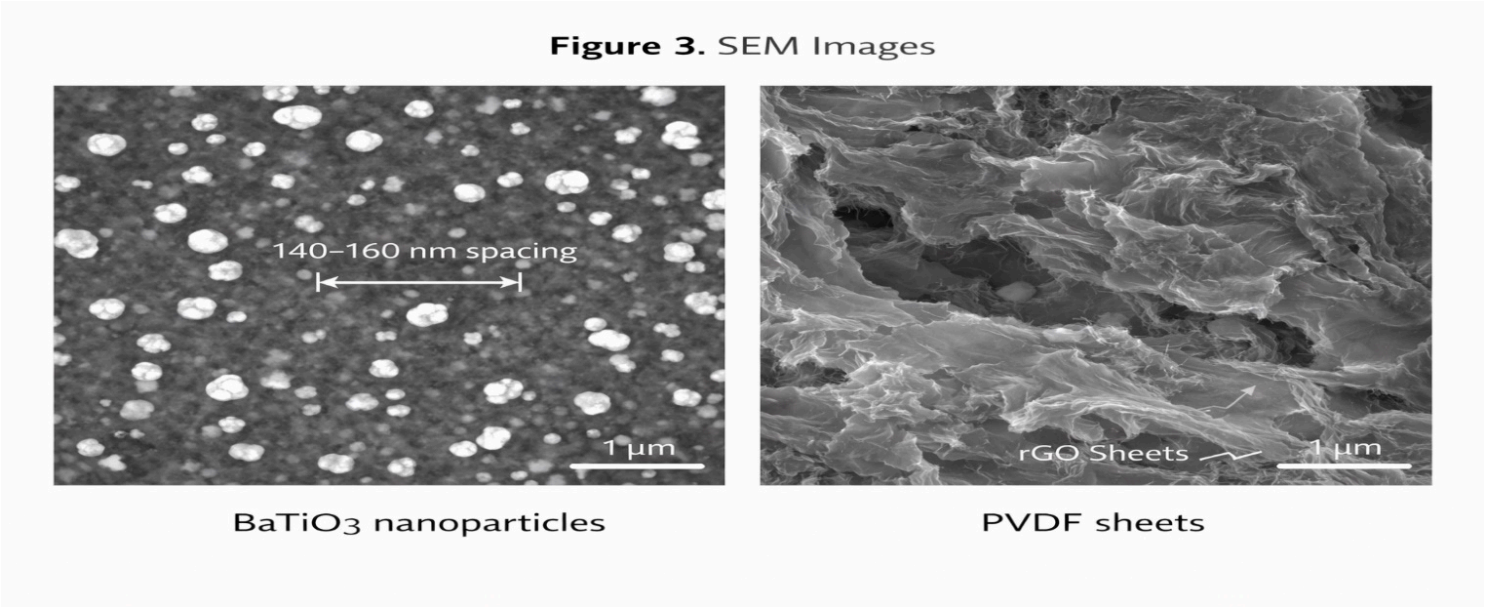

Figure 3

SEM Micrographs Showing Uniform Dispersion of $BaTiO_3$ Nanoparticles and Embedded rGO Sheets in the PVDF Matrix

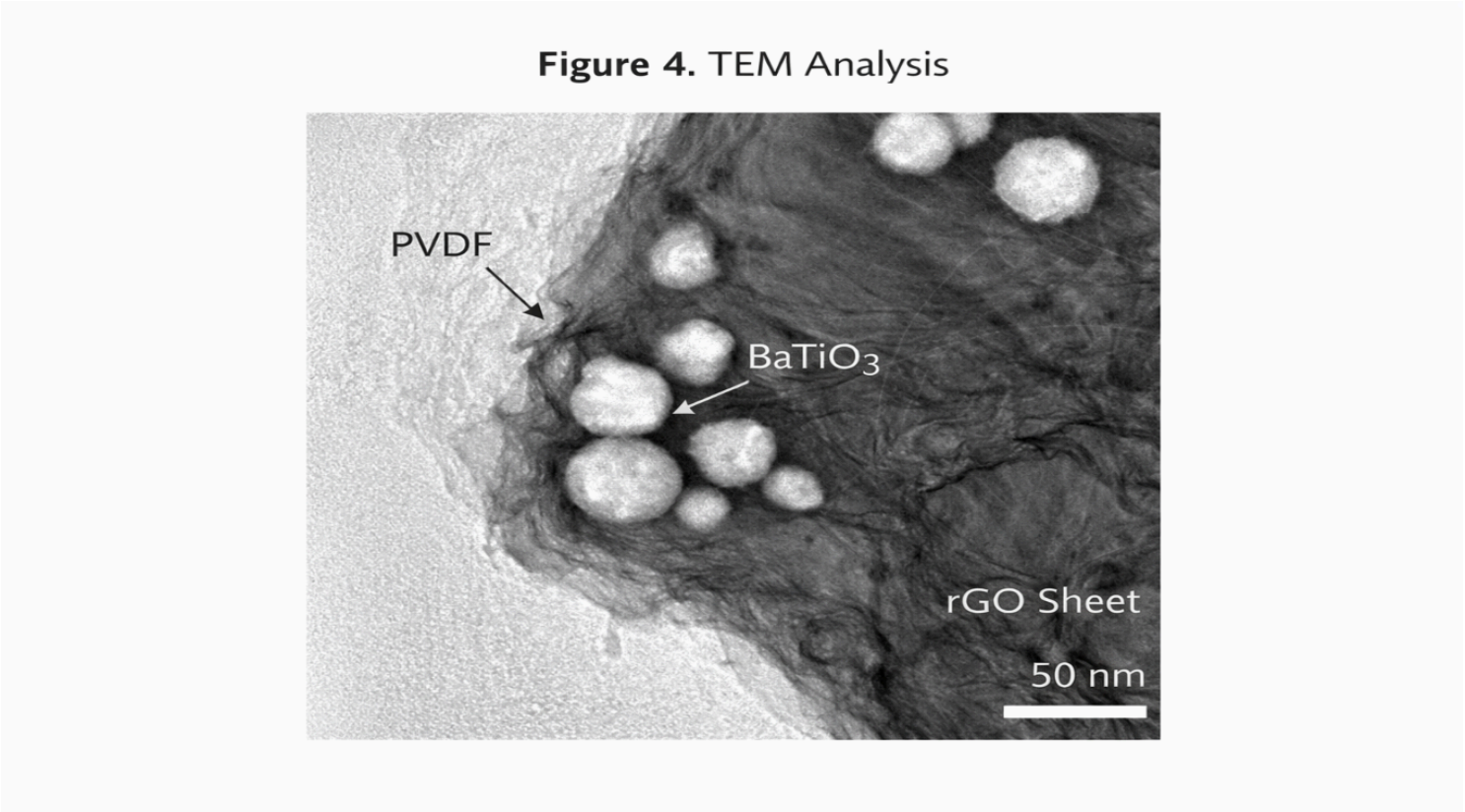

Figure 4

TEM Micrograph Showing Interfacial Adhesion and Hybrid Network Formation between $BaTiO_3$ Nanoparticles and rGO within the PVDF Matrix

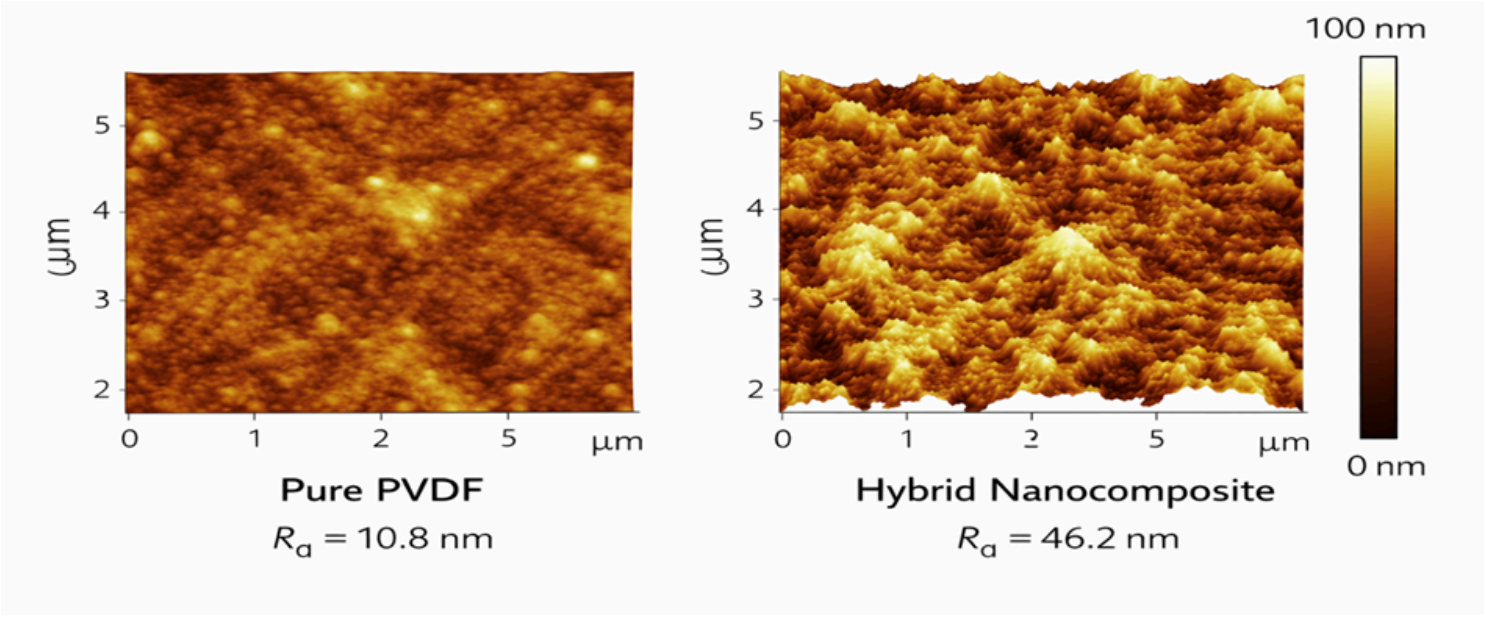

Figure 5

AFM Surface Topography Revealing Enhanced Roughness and Surface Heterogeneity in PVDF/$BaTiO_3$/Graphene Nanocomposites

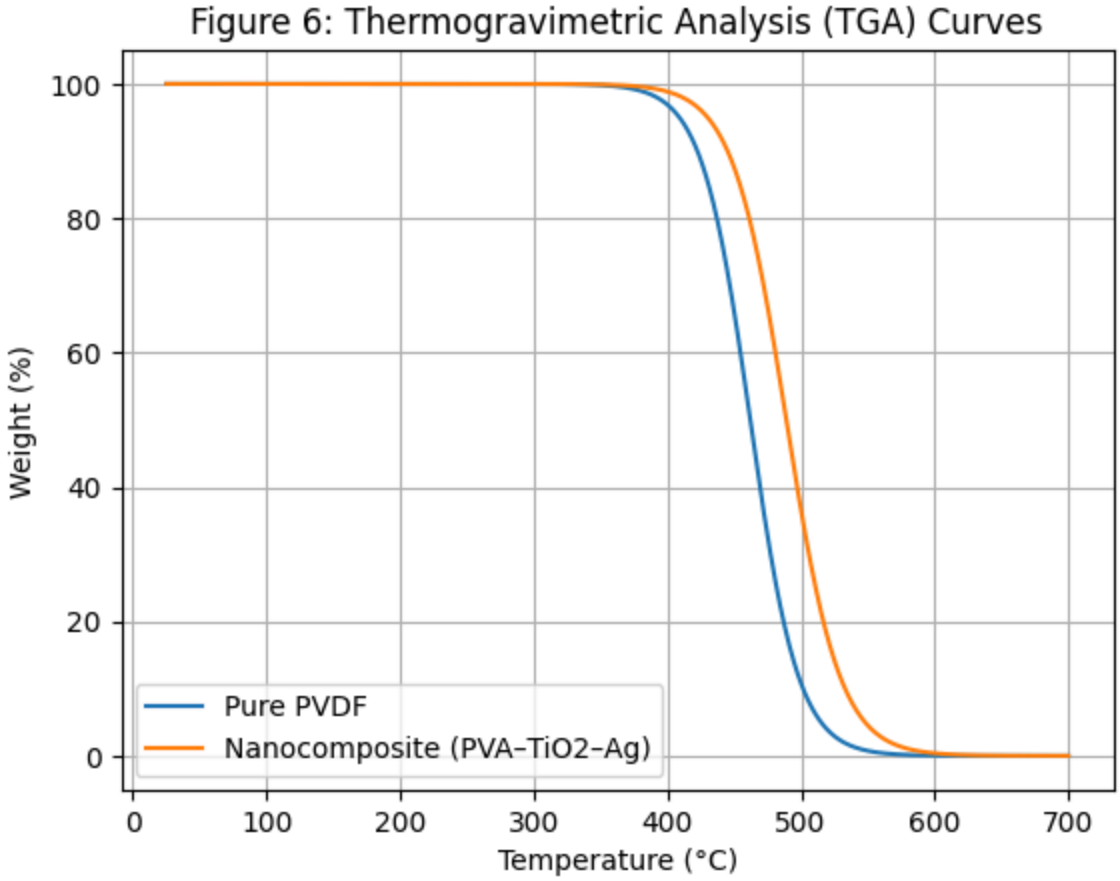

Figure 6

Thermogravimetric Analysis (TGA) of Pure PVDF and PVDF-Based Nanocomposite Showing Enhanced Thermal Stability via Interfacial Interactions

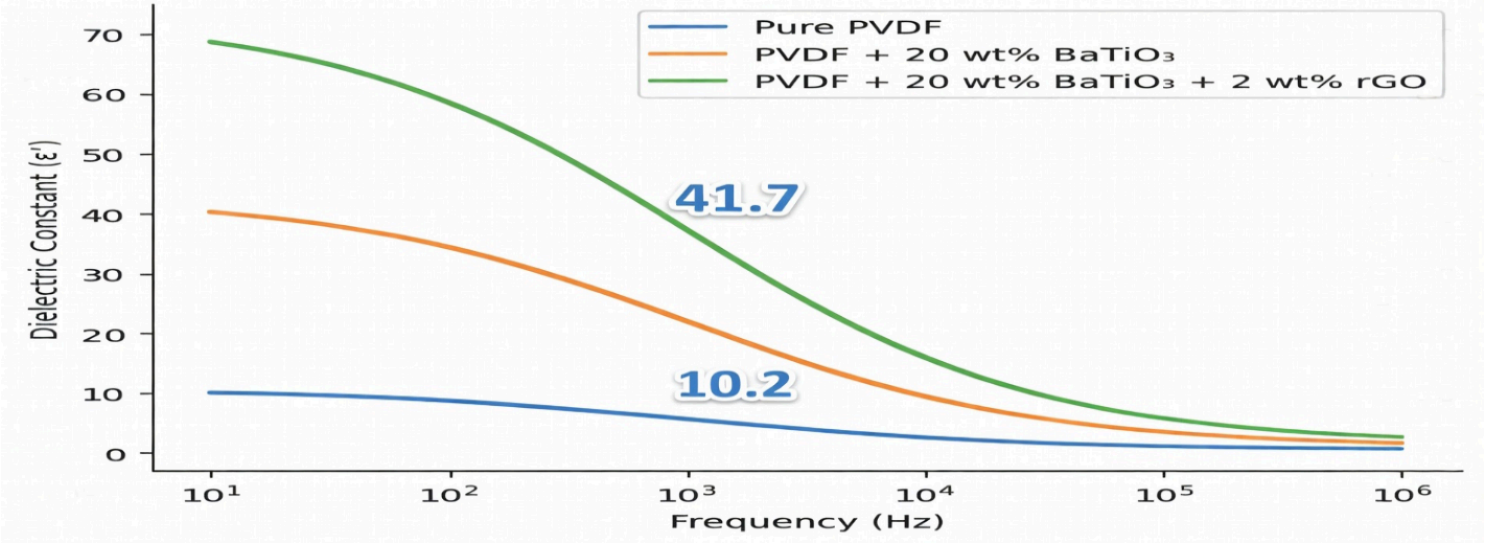

Figure 7

Frequency-Dependent Dielectric Constant of PVDF-Based Composites Highlighting Enhanced Permittivity through $BaTiO_3$ Incorporation and rGO-Induced Interfacial Polarization

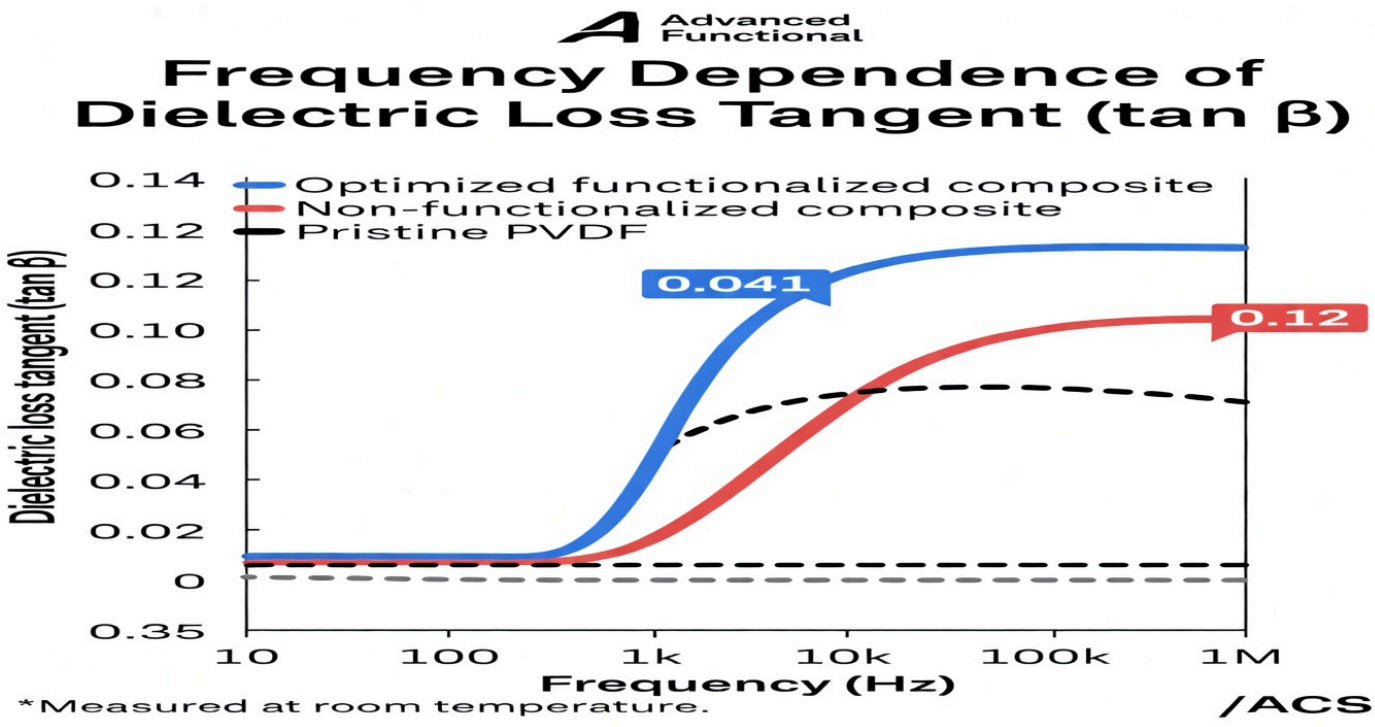

Figure 8

Frequency dependence of dielectric loss tangent (tan δ) for the optimized surface-functionalized nanocomposite, non-functionalized composite, and pristine PVDF.

Supplementary Files

This is a list of supplementary files associated with this preprint. Click to download.

- floatimage1.png